Journal of the American College of Cardiology
© 2008 by the American College of Cardiology Foundation
Published by Elsevier Inc.

Vol. 52, No. 5, 2008
ISSN 0735-1097/08/$34.00
doi:10.1016/j.jacc.2008.04.030



# Endothelial Cell Recovery Between Comparator Polymer-Based Drug-Eluting Stents

Michael Joner, MD,* Gaku Nakazawa, MD,† Aloke V. Finn, MD,‡ Shawn Chin Quee, MS,§ Leslie Coleman, DVM,§ Eduardo Acampado, DVM,† Patricia S. Wilson, BA,† Kristi Skorija, BS,† Qi Cheng, MD,† Xin Xu, PHD,† Herman K. Gold, MD,‖ Frank D. Kolodgie, PHD,† Renu Virmani, MD, FACC†¶

*Munich, Germany; Gaithersburg, Maryland; Atlanta, Georgia; Santa Clara, California; Boston, Massachusetts; and Orangeburg, New York*

**Objectives** The purpose of this study was to assess trends in endothelial coverage and recovery among leading polymer-based drug-eluting stents (DES).

**Background** Autopsy studies of human U.S. Food and Drug Administration (FDA)–approved DES implanted coronary arteries suggest that complications of late stent thrombosis are associated with incomplete endothelial coverage of struts.

**Methods** Rabbits received sirolimus-eluting stents (SES), paclitaxel-eluting stents (PES), zotarolimus-eluting stents (ZES), and everolimus-eluting stents (EES) for 14 or 28 days along with MULTI-LINK (ML) Vision control stents. Endothelial coverage above and between struts was measured by morphometric analysis of images acquired through en face scanning electron microscopy. Dual fluorescent immunolabeling was performed for platelet-endothelial cell adhesion molecule (PECAM)-1 and thrombomodulin (TM), factors involved in cell-to-cell contact and thrombogenicity, respectively. In a separate analysis, the endothelial mitogen, vascular endothelial growth factor (VEGF), was also assessed.

**Results** Varying rates of endothelialization among comparator DES were most notable at 14 days, where coverage above struts remained poor in SES, PES, and ZES (≤30%) relative to EES and ML Vision controls (≥70%), whereas no significant differences were observed at 28 days. Select DES with poor endothelialization showed a further reduced expression of PECAM-1. All DES showed an absence or weak expression of the antithrombotic cofactor TM. Incomplete endothelialization in select DES was further associated with increased VEGF secretion and messenger ribonucleic acid levels at 14 days, providing evidence of a transitional healing surface.

**Conclusions** The present study marks the first comparator analysis of endothelial coverage in leading polymeric DES, supporting disparities in arterial healing based on endothelial regrowth and recovery, favoring newer designs over the current generation of FDA-approved stents. (J Am Coll Cardiol 2008;52:333–42) © 2008 by the American College of Cardiology Foundation

Incomplete endothelialization of strut surfaces is a recognized pathologic substrate for late stent thrombosis, an infrequent but life-threatening complication of the current U.S. Food and Drug Administration (FDA)–approved drug-eluting stents (DES) (1–3). Although the underlying mechanisms of late stent thrombosis are poorly understood, endothelial regrowth is an essential component for the maintenance of long-term luminal patency because these cells provide critical structural and antithrombotic functions.

Short of large randomized clinical trials statistically powered for late thrombotic endpoints or through indirect methods for assessing endothelial dysfunction such as nitric

From the *German Heart Center, Munich, Germany; †CVPath Institute, Inc., Gaithersburg, Maryland; ‡Cardiology Division, Emory University, Atlanta, Georgia; §Abbott Vascular, Santa Clara, California; ‖Cardiac Unit, Department of Internal Medicine, Massachusetts General Hospital, Boston, Massachusetts; and the ¶Jack H. Skirball Center for Cardiovascular Research, Orangeburg, New York. This study is supported in part by a grant from Abbott Vascular, Santa Clara, California. Dr. Virmani has received company-sponsored research support from Medtronic AVE, Abbott Vascular, W.L. Gore, Atrium Medical Corporation, Boston Scientific, NDC Cordis Corporation, Novartis, Orbus Medical Technologies, Biotronik, BioSensors, Alchimer, and Terumo, and is a consultant for Medtronic AVE, Guidant, Abbott Laboratories, W.L. Gore, Terumo, and Volcano Therapeutics Inc. Drs. Chin Quee and Coleman are employees of Abbott Vascular, Santa Clara, California. Drs. Joner and Nakazawa contributed equally to this article.

Manuscript received July 2, 2007; revised manuscript received April 23, 2008, accepted April 29, 2008.

JACC Vol. 52, No. 5, 2008
July 29, 2008:333–42

**Abbreviations and Acronyms**

**DES** = drug-eluting stent(s)
**EES** = everolimus-eluting stent(s)
**FDA** = Food and Drug Administration
**PECAM** = platelet-endothelial cell adhesion molecule
**PES** = paclitaxel-eluting stent(s)
**SEM** = scanning electron microscopy
**SES** = sirolimus-eluting stent(s)
**TM** = thrombomodulin
**VEGF** = vascular endothelial growth factor
**ZES** = zotarolimus-eluting stent(s)

oxide bioavailability assays in humans (4,5), comparative preclinical histological studies remain the most effective means of evaluating healing of vascular stent implants. Although arterial repair after stent placement in animals occurs more rapidly than in humans, animal models still retain predictive value because the sequence of biological responses are remarkably similar to humans (6). The interpretation of animal data is, however, highly contingent on the timeline after stent placement. Although examination of DES implants in swine or rabbits is often done at 28 days, it is unclear whether an earlier time point may reveal more about the healing characteristics of different devices because 28 days is thought to be equivalent to 12-month coronary stent implants in humans (6,7).

Disparities in the degree of arterial healing among species is equally notable for rates of re-endothelialization after vascular injury (8,9), in which differences in shear stress, underlying atherosclerosis, and the use of juvenile animals are thought to play a role. Therefore, pre-clinical studies reporting complete endothelialization of DES at 28 and 90 days (10–12) in the porcine model failed to predict the complication of late stent thrombosis attributed to the lack of strut coverage in man after bare-metal stent (BMS) implants (2,3). Relative to porcine coronary stent implants, endothelial regrowth in the rabbit occurs at a slower rate, perhaps offering a more desirable model for assessing re-endothelialization of DES (7).

Despite worldwide use of DES in millions of patients to reduce the risk for in-stent restenosis, little, however, is known of rates of endothelialization and recovery in commercially available comparator stents. Therefore, the present study was undertaken to assess re-endothelialization with focus on surface coverage and relevant mitogenic and antithrombotic properties among leading polymer-based stent platforms.

## Methods

**Rabbit model of stent implantation.** The study protocol was reviewed and approved by the Institutional Animal Care and Research Committee, Jack H. Skirball Center for Cardiovascular Research (Orangeburg, New York), and experiments were conducted according to the National Institutes of Health Guide for the Care and Use of Laboratory Animals.

Anesthetized adult male New Zealand White rabbits underwent endothelial denudation of both iliac arteries using an angioplasty balloon catheter (3.0 × 10 mm, Abbott Vascular, Santa Clara, California). Subsequently, Cypher (Sirolimus, Cordis Corp., Johnson & Johnson, Miami, Florida), Taxus Liberté (Paclitaxel, Boston Scientific, Natick, Massachusetts), Endeavor (Zotarolimus, Medtronic Vascular, Santa Rosa, California) and XIENCE V (Everolimus, Abbott Vascular) were deployed at a target stent-to-artery ratio of 1.3:1. Bare-metal cobalt-chromium MULTI-LINK (ML) Vision stents (Abbott Vascular) served as controls (Table 1). Rabbits were anticoagulated with aspirin (40 mg/day) given orally 24 h before catheterization with continued dosing throughout the in-life phase of the study, whereas single dose intra-arterial heparin (150 IU/kg) was administered at the time of catheterization. After device implantation, post-procedural angiography was performed to document vessel patency and the animals were allowed to recover.

**Stent harvest.** The stents were harvested at 14 or 28 days after implantation. For evaluation of endothelial coverage, the stented arteries were fixed in situ with 10% neutral buffered formalin after perfusion with lactated Ringer's solution to remove blood. The samples were further fixed by immersion and then bisected longitudinally with one half processed for scanning electron microscopy (SEM) and the opposite reserved for en face immunostaining of whole-mount vessels. The adjacent proximal and distal nonstented segments served as a positive control for immunostaining.

Stents harvested for organoid culture or messenger ribonucleic acid (mRNA) extraction were immediately removed after perfusion with lactated Ringer's solution and placed in culture media or snap-frozen in liquid nitrogen, respectively, without fixation.

**Table 1** Polymer-Based Comparator Drug-Eluting and MULTI-LINK Vision Bare-Metal Stent

| Stent Design | Strut Thickness (mm) | Polymer | Polymer Thickness (mm) | Drug (Dose) | Total Dose ($\mu$g) | Release Kinetics (28 Days) |
|---|---|---|---|---|---|---|
| Cypher | 140 | PEVA+PBMA | 12.6 | Sirolimus (1.4 $\mu$g/mm$^2$) | 135 | 68.4% |
| Taxus Liberté | 97 | SIBBS | 16 | Paclitaxel (1.0 $\mu$g/mm$^2$) | 85 | 10% |
| Endeavor | 91 | PC | 5.3 | Zotarolimus (10 $\mu$g/mm) | 120 | 95%* |
| XIENCE V | 81 | Fluoropolymer | 7.6 | Everolimus (1.0 $\mu$g/mm$^2$) | 56 | 80% |
| MULTI-LINK Vision | 81 | — | — | — | — | — |

*Represents 14 days.
PC = phosphorylcholine; PEVA+PBMA = polyethylene-co-vinyl acetate + poly n-butyl methacrylate; SIBBS = poly(styrene-b-isobutylene-b-styrene).

**Morphometric analysis of endothelial surface coverage.** Composites of serial en face SEM images acquired at low power (×15 magnification) were digitally assembled to provide a complete view of the entire luminal stent surface. The images were further enlarged (×200 magnification), allowing direct visualization of endothelial cells. The extent of endothelial surface coverage above and between stent struts was traced and measured by morphometry software (IPLab for Mac OS X, Scanalytics, Rockville, Maryland). The results are expressed as a percentage of total surface area above or between struts or the total and percent area lacking coverage at each repeated crown along the longitudinal axis from proximal to distal orientation. Endothelial cells were identified as sheets of spindle or polygonal shaped monolayers in close apposition, a distinguishing feature from other cell types in en face preparations (13,14). In contrast, intimal smooth muscle cells show elongated processes and are generally stacked in disorganized or haphazard layers. Other adherent cells present on stent surfaces include platelets, characteristically 1 to 2 $\mu$m in size with an irregular discoid appearance, and inflammatory cells, which are round in shape varying from 7 to 10 $\mu$m in diameter with a ruffled surface. Struts uncovered by endothelium were completely bare or contained thrombi consisting of focal platelet and fibrin aggregates intermixed with red blood cells and inflammatory cells.

**Whole-mount en face immunostaining for platelet-endothelial cell adhesion molecule (PECAM)-1 and thrombomodulin.** Immunostaining of whole-mount specimens was achieved by overnight incubation in an antibody cocktail containing primary antibodies against PECAM-1 (CD31, 1:20 dilution, Dako, Carpentaria, California) and thrombomodulin (TM) (1:10, American Diagnostica, Stamford, Conneticut) at 4°C. Specific binding was visualized using a secondary antibody cocktail consisting of donkey-anti mouse Alexa Fluor 488 and donkey-antigoat Alexa Fluor 555 conjugate antibodies (1:200 dilution, Invitrogen Corp., Carlsbad, California); TOTO-3 iodide served as a nuclear counterstain.

The extent of endothelial coverage based on a positive reaction to PECAM-1 above and between stent struts was visually semiquantified ×100 magnification for each level of struts and expressed as a mean percentage for the total area above and between stent struts for the entire stented surface. Thrombomodulin expression was assessed based on reaction intensity ranging from an absence to strong staining relative to nonadjacent control segments. Final confocal images were acquired in a multitrack mode in which separate green or red channels were scanned individually and then superimposed using the Zeiss LSM software, thereby eliminating potential spectral overlap.

**Production of vascular endothelial growth factor (VEGF) from stents maintained in organoid culture.** Select 14- and 28-day stents harvested for organoid culture were perfused in situ with lactated Ringer's solution. The stents were then immediately transferred to 3-ml serum-free Dulbecco modified Eagle medium and maintained at 37°C in a humidified atmosphere of 5% $CO_2$/95% air. After 48 h, the conditioned medium was collected and total VEGF was measured by enzyme-linked immunosorbent assay (EMD Bioscience Inc., San Diego, California). The kit recognizes the diffusible VEGF-A isoforms of $VEGF_{165}$ and $VEGF_{121}$.

**Ribonucleic acid (RNA) extraction and reverse transcription.** The total RNA from competitor stents was isolated using TRI reagent (Applied Biosystems, Austin, Texas) followed by cleaning with RNeasy mini kit (Qiagen, Valencia, California). The isolated RNA was treated with RNase-free DNase I to remove genomic deoxyribonucleic acid according to the Qiagen protocol. The total RNA samples were quantified using Nanodrop spectrophotometry (Wilmington, Delaware), and the quality of each RNA sample was validated by measuring the A260/A280 ratio with Nanodrop and RNA integrity number (RIN) with a RNA nano 6000 Labchip kit and Agilent Bioanalyzer (Santa Clara, California).

First-strand complementary (c)DNA was synthesized from 1 $\mu$g RNA using random hexamers and MultiScribe Reverse Transcriptase in a final volume of 20 $\mu$l according to manufacturer's instructions (Applied Biosystems). The cDNA products were diluted 25-fold with nuclease-free water before use.

**Quantitative real-time polymerase chain reaction (Q-PCR).** Q-PCR was performed with SYBR green detection reagent (SuperArray, Frederick, Maryland) by using ABI 7500 fast real time PCR system (Applied Biosystems, Foster City, California). Each reaction contained 1$\mu$l cDNA template. All samples were performed in duplicate or triplicate conditions with the thermal cycling profile consisting of three stages: 95°C for 10 min, 40 cycles of 15 s at 95°C and 60°C for 1 min, followed by a dissociation curve program.

Gene-specific primers were designed using Primer Express 3.0 software (Applied Biosystems). Primer specificity was confirmed by the dissociation curve, which contained only a single peak.

Primers for PCR (5'-3'):

18S forward: GCA GCC AGG AAT AAT GGA ACA G
18S backward: GCC TCA GTT CCG AAA ACC AA
VEGF forward: CCA TGG CAG AAG AAG GAG ACA
VEGF backward: CGC CGG TAG ACT TCC ATG A

The PCR amplification efficiencies and the threshold cycle (Ct) value of each gene were determined by instrument's software. Relative expression of mRNA was calculated using the delta-delta Ct method, which involves comparing Ct values between tested samples. The internal reference gene of 18S rRNA was used to normalize the amount of RNA from all samples based on its consistent expression in rabbits relative to the housekeeping genes, glyceraldehyde 3-phosphate dehydrogenase or $\beta$-actin (15). The relative expression of target genes was presented as fold

change with the control bare-metal ML Vision stent as calibrator (ML Vision equal to 1).

**Statistical analysis.** Data are expressed as means ± SD. Multiple group comparisons were achieved using a 1-way analysis of variance (ANOVA). If the variance ratio test (F test) was significant, post hoc analysis of differences between-groups means were made using the Dunnett test. The BMS group was used as a control and compared with various DES in Dunnett tests. A p value of $<0.05$ was considered statistically significant.

## Results

**Endothelial coverage of ML Vision control stents at various intervals.** Preliminary studies determining the time course of re-endothelialization were performed in 22 rabbit iliac arteries with bare-metal ML Vision stents deployed for 3, 7, 14, and 28 days. The stents were analyzed by methods of scanning and confocal microscopy, as described earlier. Re-endothelialization by SEM showed 79.9 ± 7.4% of strut surfaces covered at 14 days, with complete overlay by 28 days (7). The percentage of PECAM-1–positive endothelial cells over struts followed similar trends with 76.6 ± 34.2% of covered strut surfaces at 14 days and >95% by 28 days. Based on this preliminary analysis, re-endothelialization of comparator DES and BMS were studied at 14 and 28 days.

**Comparator DES and ML Vision control implants.** The extent of endothelial regrowth examined by SEM and dual immunostaining against PECAM-1 and TM was assessed in a total of 96 bilateral DES and BMS (4 to 6 stents per group) implanted in 48 rabbits for 14 and 28 days. In separate experiments, an additional 80 DES and BMS (4 per group) were implanted in 40 rabbits at similar time points for analysis of VEGF release in organoid culture and mRNA expression. The stent-to-artery ratios at the time of implant were similar among groups (SES = 1.4 ± 0.17, PES = 1.4 ± 0.30, ZES = 1.2 ± 0.49, EES = 1.3 ± 0.05, and ML Vision control stent = 1.2 ± 0.12, p = NS). All animals survived the in-life phase of the study, and there were no complications of catheterization. All stents were angiographically patent at the time of euthanasia without evidence of migration or aneurysm formation.

**Endothelial coverage by SEM.** At 14 days, re-endothelialization above struts was variable among comparator stents with significantly greater coverage in EES (64.0 ± 27.5%), followed by ZES (30.2 ± 14.2%), PES (26.8 ± 15.8%), and SES (6.4 ± 4.2%), versus EES ($p < 0.003$) and ML Vision control stents ($p < 0.0001$) (Figs. 1A and 2). In contrast, areas between struts showed >70% of surface area coverage for all DES, which was most complete in EES (90.4 ± 12.4%) compared with ZES (80.6 ± 9.7%), PES (74.1 ± 16.6%), or SES (72.1 ± 9.6%) with borderline significance between groups (p = 0.08). Struts lacking endothelial coverage, as in SES and PES, generally showed focal aggregates of platelets and inflammatory cells, including giant cells. To a limited degree, adherent inflammatory cells and platelets were also found on endothelial surfaces, but no differences were noted between comparator DES (data not shown).

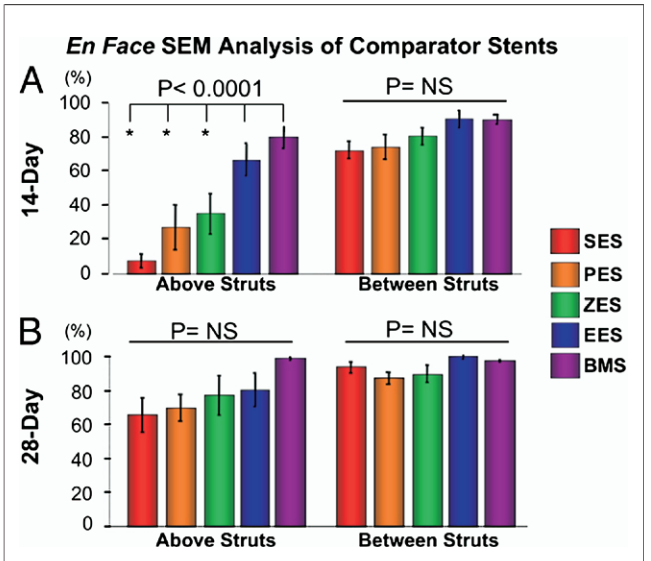


**Figure 1** Quantitative Analysis of Endothelial Coverage Based on Morphometric Analysis

Bar graphs showing the quantitative analysis of endothelial coverage above **(left)** and between struts **(right)** at 14 **(A)** and 28 days **(B)**. Comparator drug-eluting stents (DES) and bare-metal MULTI-LINK Vision control stents (BMS) based on morphometric analysis of images from scanning electron microscopy (SEM). EES = everolimus-eluting stents; PES = paclitaxel-eluting stents; SES = sirolimus-eluting stents; ZES = zotorolimus-eluting stents.

At 28 days, endothelial coverage above struts was >60% with borderline differences among comparator SES and PES versus ML Vision controls (Figs. 1B and 3). Areas above struts lacking endothelial cells showed persistent inflammatory cells and platelets/fibrin on bare surfaces. Inflammatory cells were also present in EES and ZES, however, mostly on uncovered stent struts. In comparator DES (in particular in SES and PES), rare macrophages were seen in intercellular spaces created by poorly formed cell–cell contacts.

**Total and distribution of uncovered struts among comparator DES.** Notable differences in total surface area and percent distribution of uncovered struts along the longitudinal crown structures from proximal to distal were found among 14- and 28-day comparator DES and ML Vision control stents (Fig. 4). The least area of uncovered struts was observed in ML Vision control stents (0.85 ± 0.90 $mm^2$ and 0.12 ± 0.12 $mm^2$) at 14 and 28 days, respectively. Among 14-day DES, the area of uncovered struts was least in EES, representing an approximate 2- to 3-fold increase over ML Vision controls (Fig. 4A). In contrast, there was at least a 5-fold increase in the area of uncovered struts in SES, PES, and ZES, reaching statistical significance over ML Vision ($p < 0.0001$). At 28 days, the total area of uncovered struts decreased approximately 50% in all DES with a

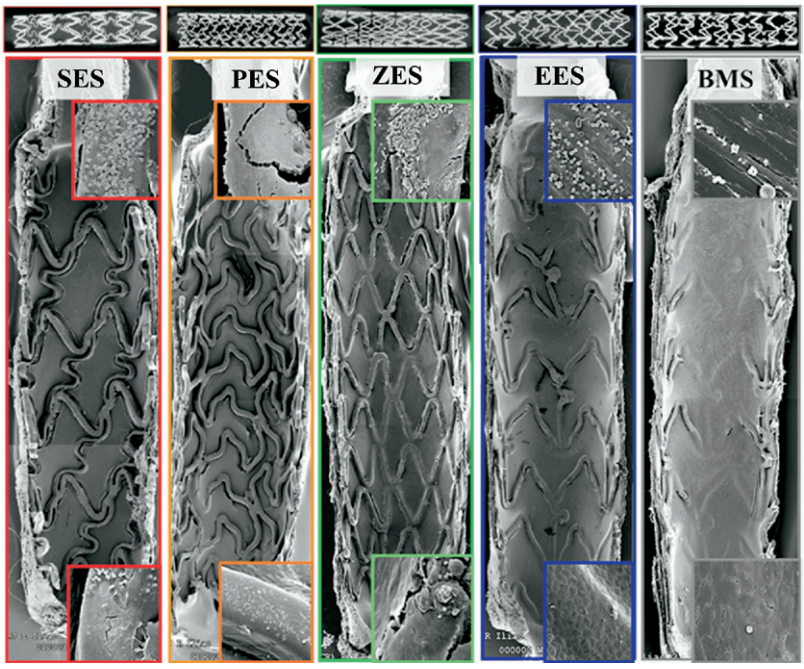


**Figure 2** **Scanning Electron Micrographs of 14-Day Comparator DES and BMS Controls**

The **upper panels** show corresponding radiographic images of each stent. The lumens are clearly patent and struts are easily discerned underneath a thin neointimal surface. Among DES, there is less endothelial cell surface coverage in SES and PES stents compared with ZES and EES. The **panel insets** are representative images at higher magnification (×200) from proximal and distal regions showing bare struts, surface thrombi, inflammatory cells, and endothelial cells. Abbreviations as in Figure 1.

persistent increase in uncovered struts in PES and SES over ML Vision controls, with the latter approaching only borderline significance.

Along the longitudinal axis, the percentage of uncovered area at each strut was more prevalent in the middle regions of all stents, producing a bell-shaped curve, as the extreme ends of the stents were generally well covered except for SES, which showed a general lack of coverage (Fig. 4B). This trend remained apparent at 28 days, although the percent area of uncovered struts was markedly less, specifically for SES, PES, and ZES; however, uncovered struts in the mid portions of all DES remain poor while the percentage of uncovered struts in ML Vision control stents was minimal (Fig. 4B).

**Endothelial monolayer integrity by PECAM-1 immunostaining.** Among DES, areas of endothelial cells with PECAM-1 localized to cell-to-cell contact sites above struts were significantly greater for EES (45.9 ± 35.6), followed by PES (21.3 ± 11.8), ZES (7.4 ± 10.2), and SES (5.8 ± 5.8), whereas 14-day ML Vision control stents showed the largest extent of coverage (55.89 ± 30.2) (Figs. 5A and 6A). Percentages of cells expressing PECAM-1 between struts were similar in EES, PES, and control ML Vision stents, which were relatively higher than SES and ZES ($p = 0.008$). The trends in PECAM-1 staining were similar to SEM findings, although the percent coverage was consistently less by PECAM-1, suggesting an overall decreased maturation of junctional complexes within stents. At 28 days, PECAM-1 staining above struts was similar for EES (67.5 ± 35.8) and ZES (64.3 ± 35.8), but less than ML Vision controls (88.1 ± 22.1), whereas in PES and SES, areas positive for PECAM-1 were <50% (Figs. 5B and 6B). There were no significant differences among DES groups between stent struts at this time point (Fig. 5B).

**Thrombomodulin immunostaining.** In nonstented control segments, TM was diffusely distributed in the cytoplasm with variable expression localized at intercellular boundaries with PECAM-1 (Figs. 6A2 and 6A3). Despite varying degrees of endothelial coverage at 14 and 28 days, TM was absent or only weakly expressed (Fig. 6B), irrespective of DES. In contrast, endothelial staining for TM showed mild to moderate intensity in ML Vision control stents at 14 and 28 days, respectively, but did not achieve the intensity of control nonstented segments.

**VEGF release from stented arterial segments in organoid culture and mRNA levels by quantitative PCR.** Analysis of conditioned media collected from 14-day stented arterial segments maintained in organoid culture over 48 h showed a 3- to 4-fold increase in VEGF release in SES, PES, and ZES relative to EES and ML Vision control stents (Fig. 7). The persistent release of VEGF in select DES was also observed at 28 days with similar trends noted. The Q-PCR analysis of 14-day stents revealed a parallel increase of VEGF mRNA levels consistent with those DES with

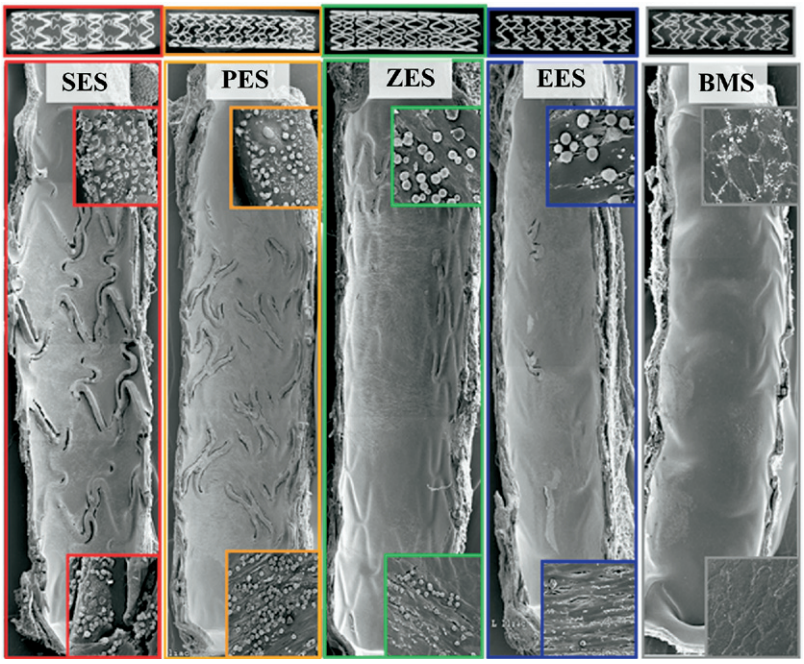


**Figure 3** **Scanning Electron Micrographs of 28-Day Comparator DES and BMS Controls**

The **upper panels** show corresponding radiographic images of each stent. The lumens are patent and struts are less discernable under a thicker neointima relative to 14-day stents. Overall endothelial coverage is near complete in all DES although it remains poor above struts in PES and SES compared with ZES and EES. The **panel insets** are at higher magnification (×200) from the proximal and distal regions and show persistent uncovered struts, surface thrombi, inflammatory cells, and endothelial cells. Abbreviations as in Figure 1.

higher amounts of VEGF. At 28 days, however, VEGF mRNA transcription was equivalent among all stents.

In separate experiments of subconfluent human umbilical vein endothelial cells treated with paclitaxel or sirolimus ($IC_{50}$ range), increased VEGF mRNA production was found at 96 h over baseline, whereas control cells treated with saline showed a reciprocal decrease (data not shown).

## Discussion

The present study marks the first comparator analysis of endothelial surface coverage in various polymeric DES using a well-characterized rabbit model of iliofemoral artery stenting (16). Endothelial coverage between struts occurred more rapidly than above struts, where differences in the various stent platforms were most notable at 14 days. In the rabbit, EES and ML Vision control stents showed a greater extent of endothelial coverage above struts relative to the current generation of FDA-approved stents (i.e., ZES, PES, and SES) at 14 days but not at 28 days. Further, there was reduced expression of PECAM-1 at cell-to-cell contacts evidenced by discontinuous or lack of immunostaining in 14-day SES, PES, and ZES, compared with EES and ML Vision control stents. This finding persisted at 28 days despite more apparent endothelial coverage by SEM analysis, suggesting delayed maturation or increased turnover of endothelial cells. Stent surfaces showed minimal endothelial expression of TM in all DES relative to ML Vision control stents, whereas it remained strongly positive in adjacent nonstented segments. Increased VEGF secretion and mRNA levels correlated with delayed endothelialization in 14-day SES, PES, and ZES in contrast to EES and ML Vision control stents, where endothelial coverage was more complete. The increased VEGF release persisted at 28 days, further providing evidence of a transitional immature endothelial surface in select DES.

**Factors responsible for delayed endothelial regrowth in DES.** Intuitively, the disparity of endothelial coverage above and between struts partially arises from physical contact, where strut surfaces provide greater injury and drug exposure, whereas inter-struts areas are exposed to less injury and lower concentrations of drug (17). Consistent with BMS, endothelial regrowth seems to arise from intact endothelium adjacent to the injured site as it divides and migrates to reline the arterial surface (18). This finding is consistent in the present study, in which endothelial coverage was generally more complete at the extreme proximal and distal regions of the stent versus the middle segments.

Regional differences in blood flow dictated by varying stent configurations and altered shear stresses are capable of impacting endothelial growth (19,20). Specifically, flow disturbances caused by increased strut thickness are a likely deterrent of endothelial coverage. In a seminal study under

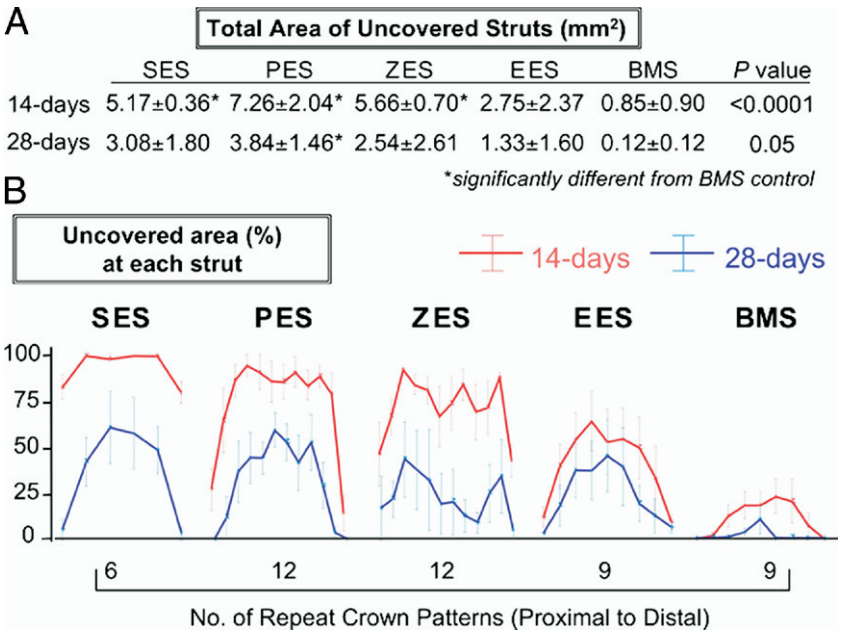


**Figure 4** **Morphometric Analysis of Uncovered Strut Area (mm²) Among Comparator DES and BMS Control Stents**

The summary table **(A)** shows the total area (mm²) of uncovered struts was significantly greater in SES, PES, and ZES compared to MULTI-LINK Vision, especially at 14 days. **Panel B** represents a series of line graphs representing the quantitative distribution of uncovered struts at each repeat *crowns* along the longitudinal axis of the stent from proximal to distal. Uncovered struts were more prevalent in the middle regions of most stents, except for SES at 14 days where uncovered struts were prominent along the entire stent length. Analysis of 28-day stents shows a persistent lack of strut coverage in the midsegment of SES and PES compared with BMS. Abbreviations as in Figure 1.

flow and shear conditions similar to those found in arteries, Simon et al. (21) found the extent of endothelial coverage is dependent on object thickness. After 24 h, endothelial cell coverage and maximum migration distance significantly decreased over objects ≥75 μm and was nonexistent at 250 μm. These data support previous clinical studies in which reduced arterial injury and restenosis are associated with thinner struts (22–24). Strut/polymer thickness in the present study was least in stents with greater endothelial coverage: EES (89 μm) and ZES (96 μm) compared with PES (113 μm) and SES (153 μm), where endothelial coverage was uniformly poor (Table 1).

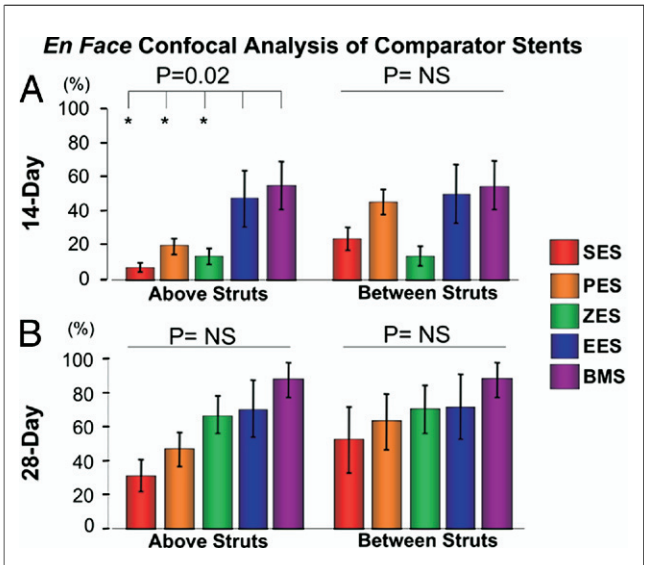


**Figure 5** **Quantitative Analysis of Endothelial Coverage Based on Immunostaining Against PECAM-1**

Bar graphs showing the quantitative analysis of endothelial coverage above **(left)** and between struts **(right)** at 14 **(A)** and 28 days **(B)**. Comparator DES and BMS based on immunostaining against platelet-endothelial cell adhesion molecule (PECAM)-1. Abbreviations as in Figure 1.

The drug dose/polymer combination and release properties may also affect endothelial cell proliferation and migration. Pharmacokinetic profiles (in vivo) for sirolimus, SES, and everolimus, EES, show 68.4%, and 79.5% of the total drug released at 28 days, respectively (11,25), whereas the majority (95%) of zotarolimus, ZES, is released by 14 days (26). Therefore, comparative release rates alone do not explain the relative increased endothelial coverage with EES, which may be secondary to a lower loading dose together with the rapid release rate. In contrast, only 10% of paclitaxel (slow-release PES) is released by 28 days, where local concentrations of this cytotoxic drug achieve therapeutic doses capable of inhibiting endothelial proliferation and migration and inducing apoptosis as well (27,28).

**Endothelial cell monolayer integrity and PECAM-1.** In the present study, we examined the expression of the endothelial antigen PECAM-1, a molecule proven critical to endothelial homeostasis. PECAM-1 is a transmembrane

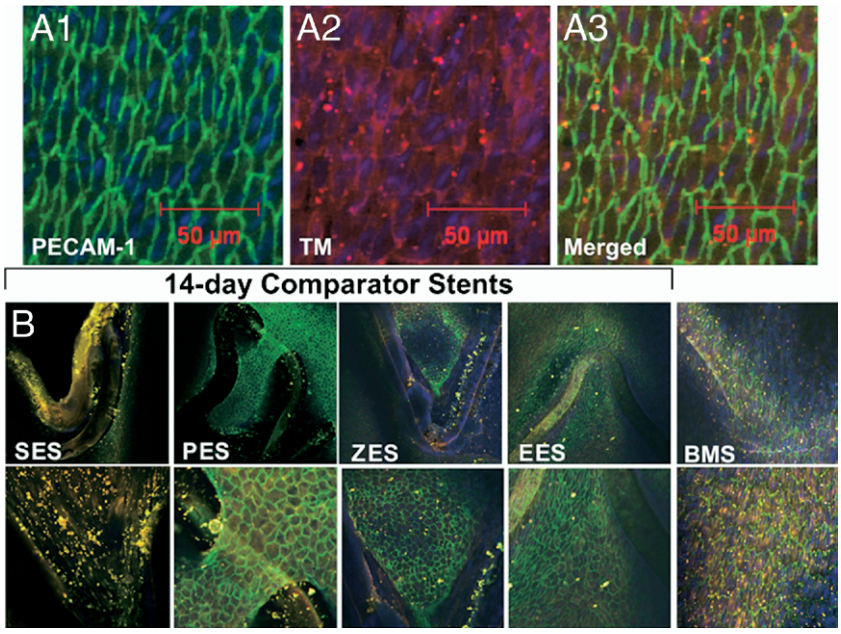


**Figure 6** **Dual Immunofluorescence for PECAM-1 and TM**

Dual immunofluorescence for PECAM-1 and thrombomodulin (TM) in whole mount control non-stented **(A1 to A3)** and stented **(B)** arterial segments. **Panel A1**, control shows strong cell-cell border localization of PECAM-1 while **panel A2** shows diffuse staining for TM with relatively weak staining at the cell periphery. The merged panel **(A3)** shows minimal fluorophore overlap **(yellow)**; TOTO-3 **(blue)** was used as a nuclear counterstain. **Panel B** represents low **(upper row)** and higher magnification **(bottom row)** merged confocal images of 14-day stents dual stained for PECAM-1 **(green)** and TM **(red)**. The extent of PECAM-1 positive endothelial cells was variable for each stent type, with more uniform expression above struts in EES and BMS. Struts with poor expression for PECAM-1 were more frequent in SES, PES, and ZES. Thrombomodulin expression was weak or absent in all DES, while mild to moderate staining was noted in BMS. Abbreviations as in Figures 1 and 5.

glycoprotein concentrated in broad areas of cell-to-cell contact where homophilic interactions with PECAM-1 of neighboring endothelial cells occur (29). Endothelial cells form poor cell junctions during processes such as cell growth and migration, displaying a loss of PECAM-1 immunostaining at endothelial margins (30,31). The extent of endothelial regrowth assessed by en face immunostaining against PECAM-1 followed similar trends as seen by SEM analysis, although area coverage was notably less in the former. In particular, PECAM-1 expression over struts in 14- and 28-day SES and PES was generally poor, suggesting an inhibition of endothelial cell migration and proliferation, endothelial injury, and/or increased cell turnover.

The expression of TM, a physiologically relevant regulator of platelets and coagulation, was also examined because the loss of TM function causes spontaneous thrombosis in the arterial and venous circulation (32). Overall staining for TM was absent or only weakly expressed in 14- and 28-day DES, and was even reduced in ML Vision control stents compared with nonstented segments. This finding may be of clinical importance because dysfunctional endothelium combined with a lack of endothelial coverage may also play a role in late stent thrombosis. No animal or human pathologic study to date has examined the expression of proteins critical to endothelial homeostasis in stents. Reduced expression of TM in DES suggests a switch to a more prothrombogenic state similar to that reported in early vein grafts in the rabbit (33,34). Moreover, the inability of DES to provide an antithrombogenic surface parallels in vitro studies in which endothelial cells treated with paclitaxel or sirolimus show increased tissue factor mRNA and protein expression (35,36). Both rapamycin and paclitaxel also selectively enhance the expression of plasminogen-activator inhibitor type I, a potent inhibitor of fibrinolysis and mediator of acute thrombosis (37).

**Integrity of the surface endothelium in DES: maintenance by VEGF.** Overexpression of VEGF accelerates endothelial repair and inhibits neointimal formation after arterial injury (38,39). Increased levels of VEGF correlate with regenerating versus quiescent endothelial cells as VEGF message and protein expression peak early after arterial injury and then diminish with greater healing (40,41). In our study, secreted VEGF and mRNA levels were highest in SES, PES, and ZES, stents with poorly endothelialized surfaces at 14 days. The persistent production of VEGF in selected DES seems to be a function of incomplete endothelialization rather than a direct effect of the drug as rapamycin, for example is reported to partially downregulate VEGF in tumors via mTORC2 (42). Although secreted VEGF correlated with increased mRNA levels at 14 days, stents harvested at 28 days showed discordant VEGF protein and mRNA levels where secreted

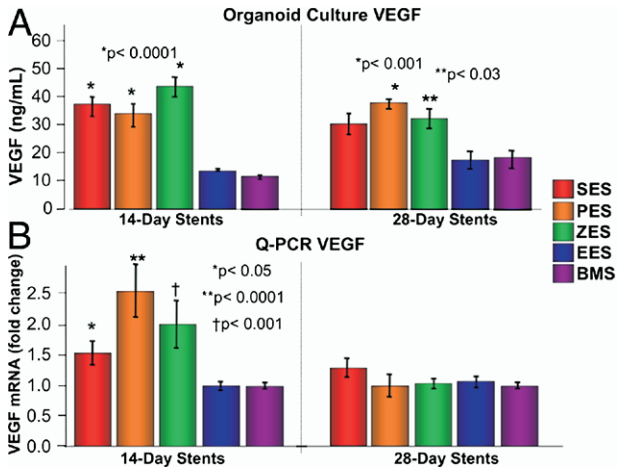


**Figure 7** **Measurement of VEGF Production and mRNA Levels by Q-PCR at 14- and 28-Day Stent Implants**

**(A)** Vascular endothelial growth factor (VEGF) secretion from stents (harvested at 14 and 28 days) maintained in organoid culture over 48 h showed a significant increase in SES, PES, and ZES relative to EES and BMS. **(B)** Concordant quantitative polymerase chain reaction (Q-PCR) analysis of VEGF messenger ribonucleic acid (mRNA) levels matches with DES showing higher released amounts of VEGF at 14 days.

VEGF from select DES was found independent of transcriptional activation. The regulatory pathways of VEGF are undoubtedly complex because differential rates of healing of various DES may effect post-translational processes involving the proteolytic release of matrix-bound and receptor-bound VEGF isoforms (43).

**Clinical implications and perspectives.** Several factors are associated with an increased risk of stent thrombosis, including the procedure itself (stent malapposition and/or underexpansion, number of implanted stents, stent length, persistent slow coronary blood flow, and dissections), patient and lesion characteristics, stent design, and discontinuation of antiplatelet drugs (44). It is important to emphasize that similar factors have been implicated in late stent thrombosis of BMS (45). Nonetheless, the apparent off-label use of DES has given rise to the ongoing debate of increased risk of late stent thrombosis in these devices (46).

Our results support an increased late thrombotic risk associated with DES relative to BMS caused by inadequate endothelial coverage over stent struts. The restoration of endothelial function within the stent may be further impaired because of an underlying dysfunctional endothelium in symptomatic plaques. Moving beyond the exuberance of curing restenosis, attention should focus on stent strut coverage rather than late loss alone because the persistent lack of coverage as reported in recent clinical (47) and autopsy (3) studies may serve as a nidus for thrombosis. Improved stent designs with thinner struts, more biocompatible polymers, or elimination of polymers with optimized drug elution profiles will likely have a profound impact on endothelial coverage, but these are slow to reach approval because they require extensive pre-clinical study and large randomized clinical trials powered for safety end points. The selection of appropriate animal models, porcine versus rabbit, may also be important for the study of endothelial regeneration.

**Study limitations.** The appropriate bare-metal control stents matched for the various DES (SES, PES, and ZES) were unavailable, thus preventing the assessment of stent configurations on re-endothelialization. Moreover, balloon denudation was performed before stenting, which can influence the degree of endothelial coverage. In the clinical setting, stent deployment without antecedent balloon denudation leaves more endothelium intact, lowering the requirement for endothelial proliferation and migration. Because all DES were tested in the iliac arteries, these results may not be directly applicable to the coronary vascular bed because of differences in shear rates.

The study of normal arteries also may not adequately represent biological responses of human atherosclerotic arteries treated with DES because pre-existing inflammation in atherosclerotic arteries may further delay healing. The impact of platelet interactions on restoration of endothelial integrity was also not addressed, as thienopyridines were not administered. Nonetheless, our rabbit model would have predicted the likelihood of late stent thrombosis with Cypher and Taxus stents. Conversely our data regarding ZES and EES falls short of predicting safety in regard to late stent thrombosis, which requires confirmation in long-term clinical trials in a large number of patients. Notably, all DES examined showed a lack of endothelial anticoagulant function independent of surface coverage.

## Conclusions

A disparity in arterial healing involving re-endothelialization of various polymeric DES in the rabbit was observed at 14 days. Endothelial coverage among DES was less discernable at 28 days, the traditional time point for analysis of stents in animals, likely caused by accelerated rates of arterial healing relative to humans. Significantly less endothelial strut coverage at 14 days was more apparent in earlier stent designs loaded with SES or PES relative to the more recent EES or ZES.

### Acknowledgment

The authors thank Lila Adams (CVPath Institute, Inc.) for her valuable technical assistance.

**Reprint requests and correspondence:** Dr. Renu Virmani, CVPath, Institute, Inc., 19 Firstfield Road, Gaithersburg, Maryland 20878. E-mail: rvirmani@cvpath.org.

### REFERENCES

1. Pfisterer M, Brunner-La Rocca HP, Buser PT, et al. Late clinical events after clopidogrel discontinuation may limit the benefit of

drug-eluting stents: an observational study of drug-eluting versus bare-metal stents. J Am Coll Cardiol 2006;48:2584–91.
2. Joner M, Finn AV, Farb A, et al. Pathology of drug-eluting stents in humans: delayed healing and late thrombotic risk. J Am Coll Cardiol 2006;48:193–202.
3. Finn AV, Joner M, Nakazawa G, et al. Pathological correlates of late drug-eluting stent thrombosis: strut coverage as a marker of endothelialization. Circulation 2007;115:2435–41.
4. Hofma SH, van der Giessen WJ, van Dalen BM, et al. Indication of long-term endothelial dysfunction after sirolimus-eluting stent implantation. Eur Heart J 2006;27:166–70.
5. Togni M, Windecker S, Cocchia R, et al. Sirolimus-eluting stents associated with paradoxic coronary vasoconstriction. J Am Coll Cardiol 2005;46:231–6.
6. Virmani R, Kolodgie FD, Farb A, Lafont A. Drug eluting stents: are human and animal studies comparable? Heart 2003;89:133–8.
7. Finn AV, Nakazawa G, Joner M, et al. Vascular responses to drug eluting stents: importance of delayed healing. Arterioscler Thromb Vasc Biol 2007;27:1500–10.
8. Dixit P, Hern-Anderson D, Ranieri J, Schmidt CE. Vascular graft endothelialization: comparative analysis of canine and human endothelial cell migration on natural biomaterials. J Biomed Mater Res 2001;56:545–55.
9. Rezvan A, Allen FD, Lelkes PI. Steady unidirectional laminar flow inhibits monolayer formation by human and rat microvascular endothelial cells. Endothelium 2004;11:11–6.
10. Suzuki T, Kopia G, Hayashi S, et al. Stent-based delivery of sirolimus reduces neointimal formation in a porcine coronary model. Circulation 2001;104:1188–93.
11. Klugherz BD, Llanos G, Lieuallen W, et al. Twenty-eight-day efficacy and phamacokinetics of the sirolimus-eluting stent. Coron Artery Dis 2002;13:183–8.
12. Goode J. FDA Summary: Taxus Express Paclitaxel-Eluting Monorail and Over-the-Wire Coronary Stent Systems-PMA for Marketing Approval. U.S. Food and Drug Administration, 2003:1–43.
13. Jamal A, Bendeck M, Langille BL. Structural changes and recovery of function after arterial injury. Arterioscler Thromb 1992;12:307–17.
14. Zand T, Nunnari JJ, Hoffman AH, et al. Endothelial adaptations in aortic stenosis. Correlation with flow parameters. Am J Pathol 1988;133:407–18.
15. Deindl E, Boengler K, van Royen N, Schaper W. Differential expression of GAPDH and beta3-actin in growing collateral arteries. Mol Cell Biochem 2002;236:139–46.
16. Finn AV, Kolodgie FD, Harnek J, et al. Differential response of delayed healing and persistent inflammation at sites of overlapping sirolimus- or paclitaxel-eluting stents. Circulation 2005;112:270–8.
17. Hwang CW, Wu D, Edelman ER. Physiological transport forces govern drug distribution for stent-based delivery. Circulation 2001; 104:600–5.
18. Rogers C, Parikh S, Seifert P, Edelman ER. Endogenous cell seeding. Remnant endothelium after stenting enhances vascular repair. Circulation 1996;94:2909–14.
19. LaDisa JF, Jr., Olson LE, Douglas HA, Warltier DC, Kersten JR, Pagel PS. Alterations in regional vascular geometry produced by theoretical stent implantation influence distributions of wall shear stress: analysis of a curved coronary artery using 3D computational fluid dynamics modeling. Biomed Eng Online 2006;5:40.
20. Richter Y, Edelman ER. Cardiology is flow. Circulation 2006;113: 2679–82.
21. Simon C, Palmaz JC, Sprague EA. Influence of topography on endothelialization of stents: clues for new designs. J Long Term Eff Med Implants 2000;10:143–51.
22. Kastrati A, Mehilli J, Dirschinger J, et al. Intracoronary stenting and angiographic results: strut thickness effect on restenosis outcome (ISAR-STEREO) trial. Circulation 2001;103:2816–21.
23. Pache J, Kastrati A, Mehilli J, et al. Intracoronary stenting and angiographic results: strut thickness effect on restenosis outcome (ISAR-STEREO-2) trial. J Am Coll Cardiol 2003;41:1283–8.
24. Rittersma SZ, de Winter RJ, Koch KT, et al. Impact of strut thickness on late luminal loss after coronary artery stent placement. Am J Cardiol 2004;93:477–80.
25. Serruys PW, Ruygrok P, Neuzner J, et al. A randomised comparison of an everolimus-eluting coronary stent with a paclitaxel-eluting coronary stent: the SPIRIT II trial. EuroIntervention 2006;2:286–94.
26. Kandzari DE, Leon MB. Overview of pharmacology and clinical trials program with the zotarolimus-eluting endeavor stent. J Interv Cardiol 2006;19:405–13.
27. Kamath KR, Barry JJ, Miller KM. The Taxus drug-eluting stent: a new paradigm in controlled drug delivery. Adv Drug Deliv Rev 2006;58:412–36.
28. Wessely R, Blaich B, Belaiba RS, et al. Comparative characterization of cellular and molecular antirestenotic profiles of paclitaxel and sirolimus. Implications for local drug delivery. Thromb Haemost 2007;97:1003–12.
29. Newton JP, Buckley CD, Jones EY, Simmons DL. Residues on both faces of the first immunoglobulin fold contribute to homophilic binding sites of PECAM-1/CD31. J Biol Chem 1997;272:20555–63.
30. Gratzinger D, Barreuther M, Madri JA. Platelet-endothelial cell adhesion molecule-1 modulates endothelial migration through its immunoreceptor tyrosine-based inhibitory motif. Biochem Biophys Res Commun 2003;301:243–9.
31. RayChaudhury A, Elkins M, Kozien D, Nakada MT. Regulation of PECAM-1 in endothelial cells during cell growth and migration. Exp Biol Med (Maywood) 2001;226:686–91.
32. Isermann B, Hendrickson SB, Zogg M, et al. Endothelium-specific loss of murine thrombomodulin disrupts the protein C anticoagulant pathway and causes juvenile-onset thrombosis. J Clin Invest 2001;108: 537–46.
33. Kim AY, Walinsky PL, Kolodgie FD, et al. Early loss of thrombomodulin expression impairs vein graft thromboresistance: implications for vein graft failure. Circ Res 2002;90:205–12.
34. Sperry JL, Deming CB, Bian C, et al. Wall tension is a potent negative regulator of in vivo thrombomodulin expression. Circ Res 2003;92:41–7.
35. Stahli BE, Camici GG, Steffel J, et al. Paclitaxel enhances thrombin-induced endothelial tissue factor expression via c-Jun terminal NH2 kinase activation. Circ Res 2006;99:149–55.
36. Steffel J, Latini RA, Akhmedov A, et al. Rapamycin, but not FK-506, increases endothelial tissue factor expression: implications for drug-eluting stent design. Circulation 2005;112:2002–11.
37. Muldowney JA, 3rd, Stringham JR, Levy SE, et al. Antiproliferative agents alter vascular plasminogen activator inhibitor-1 expression: a potential prothrombotic mechanism of drug-eluting stents. Arterioscler Thromb Vasc Biol 2007;27:400–6.
38. Asahara T, Bauters C, Pastore C, et al. Local delivery of vascular endothelial growth factor accelerates reendothelialization and attenuates intimal hyperplasia in balloon-injured rat carotid artery. Circulation 1995;91:2793–801.
39. Hutter R, Carrick FE, Valdiviezo C, et al. Vascular endothelial growth factor regulates reendothelialization and neointima formation in a mouse model of arterial injury. Circulation 2004;110:2430–5.
40. Wysocki SJ, Zheng MH, Smith A, Norman PE. Vascular endothelial growth factor (VEGF) expression during arterial repair in the pig. Eur J Vasc Endovasc Surg 1998;15:225–30.
41. Zhao Q, Ishibashi M, Hiasa K, Tan C, Takeshita A, Egashira K. Essential role of vascular endothelial growth factor in angiotensin II-induced vascular inflammation and remodeling. Hypertension 2004;44:264–70.
42. Kurmasheva RT, Harwood FC, Houghton PJ. Differential regulation of vascular endothelial growth factor by Akt and mammalian target of rapamycin inhibitors in cell lines derived from childhood solid tumors. Mol Cancer Ther 2007;6:1620–8.
43. Shenberger JS, Zhang L, Powell RJ, Barchowsky A. Hyperoxia enhances VEGF release from A549 cells via post-transcriptional processes. Free Radic Biol Med 2007;43:844–52.
44. Luscher TF, Steffel J, Eberli FR, et al. Drug-eluting stent and coronary thrombosis: biological mechanisms and clinical implications. Circulation 2007;115:1051–8.
45. Farb A, Burke AP, Kolodgie FD, Virmani R. Pathological mechanisms of fatal late coronary stent thrombosis in humans. Circulation 2003;108:1701–6.
46. Farb A, Boam AB. Stent thrombosis redux–the FDA perspective. N Engl J Med 2007;356:984–7.
47. Takano M, Inami S, Jang IK, et al. Evaluation by optical coherence tomography of neointimal coverage of sirolimus-eluting stent three months after implantation. Am J Cardiol 2007;99:1033–8.

**Key Words:** drug-eluting stents ■ endothelium ■ platelet-endothelial adhesion molecule-1 ■ vascular endothelial growth factor.